APCC
APEC CLIMATE CENTER

PREFACE

It is our pleasure to present to you the APEC Climate Center (APCC)'s Technical Report 2011, which reports the core outcomes of our research activities from the past year.

Since 2005, APCC, as a hub of climate information in the Asia-Pacific region, has strived to share our analysis and prediction of abnormal climate and to apply this information to regional development. The center has established the largest Multi-Model Ensemble (MME) system for seasonal prediction through its international science network and has provided value-added products to various stakeholders. Recently, APCC has expanded its mandate to include enhancement of the capacity of APEC member economies information to respond effectively to climate change and variability through better application of climate.

To achieve its research and social objectives, in 2011, APCC made efforts to research improvements in its climate prediction performance from various angles and towards better understanding of climate variability and the reproducibility of the climate models for the relevant application of climate information to society. The following technical report provides more information about our research outcomes from 2011.

APCC will continue to improve the quality and accuracy of climate information, recognizing that the utility of this information is only as good as its quality. We would like to make the best use of our research results for the benefit of society and academia. We also welcome any feedback on this report or on our services.

My best and warmest regards to all of you.

Dr. Chin-Seung Chung
Director/APEC Climate Center

CONTENTS

Model Evaluation for Low-Level Cloud Feedback

Dr. Sun-Hee Shin

APCC

TECHNICAL REPORT 2011-03

Model Evaluation for Low-Level Cloud Feedback

Dr. Sun-Hee Shin

ABSTRACT

The purpose of this research is to address the cloud feedback in a future climate scenario predicted using global climate models. To understand the variability of low-level clouds in the current climate, variations in cloud cover as well as relationship between cloud cover and other variables are examined using the adjusted International Satellite Cloud Climatology Project (ISCCP) data and Intergovernmental panel on climate change (IPCC) Fourth Assessment Report (AR4) models.

The study focuses on the low-level cloud amount, the variability of which is critical in balancing earth's radiation budget. The correlations of the observed low-level cloud cover anomalies with a variety of variables suggest that low-level clouds in tropical marine areas (persistent low-level cloud regions) are associated with a cool sea surface temperature, stronger stability, higher sea level pressure, and subsidence. An increase in SST causes a reduction in lower tropospheric stability, which in turn allows for more vertical motion within and around the cloud deck that leads to increased dry air entrainment. This brings about a reduction in cloudiness and a transition from low-level to high-level cloud types. Higher SLP can also produce more subsidence aloft, thereby increasing LTS independent of SST.

Obtaining a better understanding of the physical processes that control cloud response to climate variability and the evaluation of cloud feedbacks simulated by current models should help to assess which of the model estimates of cloud feedback is the most reliable. To more closely examine the evidence of low-level cloud responses, the correlations between cloud cover and various meteorological variables in the four cloud regions with persistent low-level cloud cover are computed for each model and compared with observations. Models are selected according to whether they have the correct sign of correlation relative to observations. Two models passed the cloud-meteorology correlation test, exhibiting considerably good agreement with observed net cloud radiative forcing. These models show a reduction in cloud cover throughout much of the Pacific in response to global warming by greenhouse gas forcing (i.e., a positive feedback). In this study, we give a concise answer to the question of whether low-level clouds act as a positive or negative feedback to climate change.

1. INTRODUCTION

Clouds have opposing effects on the earth's radiation budget in that they reflect solar radiation back to space (the albedo effect of clouds), but also trap thermal radiation emitted by the earth's surface (the greenhouse effect of clouds). These two effects are usually denoted as the shortwave (SW) and longwave (LW) components of cloud radiative forcing (CRF). The balance between the SW and LW effects results

in different radiative properties and depends on cloud type and attributes such as height and thickness. For example, high clouds tend to have a net warming effect because they reflect little incoming shortwave radiation (due to their thin thickness) and emit little longwave radiation towards space (due to their high altitude and resulting low temperature). Conversely, low clouds tend to produce a net cooling effect by combining a small greenhouse effect (due to their low altitude and resulting high temperature) and generally high albedo (due to thick cloud depth). Deep convective clouds, on the other hand, have almost no effect on the climate because of their strong greenhouse effect and high albedo. Therefore, for a more complete understanding of the Earth's radiation budget, we must understand how different types of clouds are distributed globally, how the cloud distribution changes with climate change.

Currently, clouds exert a net cooling effect on the climate (Fig. 1). According to the results from the International Satellite Cloud Climatology Project (ISCCP), the global mean CRF is negative, with a net radiation budget that amounted to $-24\,Wm^{-2}$ from January 1984-December 2007. Spatially, clouds generate a cooling effect except for the polar regions and certain continents (indicated with dark blue). This cooling effect is especially prominent over the subtropical marine areas and mid-latitude oceans (with red color) where low-level clouds are prevalent. The zonal mean magnitude of the cooling effect is most evident over ocean areas and seems to be proportional to the zonal mean low cloud amount. That is, low-level clouds over ocean areas contribute significantly to the overall net cooling impact of clouds on the earth's climate. The cooling effect of clouds might be enhanced or weakened through radiative feedback associated with global warming (Randall et al., 2006; NRC, 2003; Zhang, 2004; Stephens, 2005; Bony et al., 2006). Klein and Hartmann (1993) showed that a one-percent change in stratocumulus cloud cover could lead to a change in net cloud forcing at the top of the atmosphere of roughly $1\,Wm^{-2}$, whereas the change in the direct forcing caused by doubled CO_2 is estimated to be $4\,Wm^{-2}$. This result suggests that a moderate change in low-level clouds can markedly offset or amplify global warming due to increasing greenhouse gases depending on the sign of cloud feedbacks (Slingo, 1990). Since low-level clouds are the major contributor to CRF, it is important to document how a change in the

climate may affect low-level clouds and modulate the impact of cloud cover on the Earth's radiation budget.

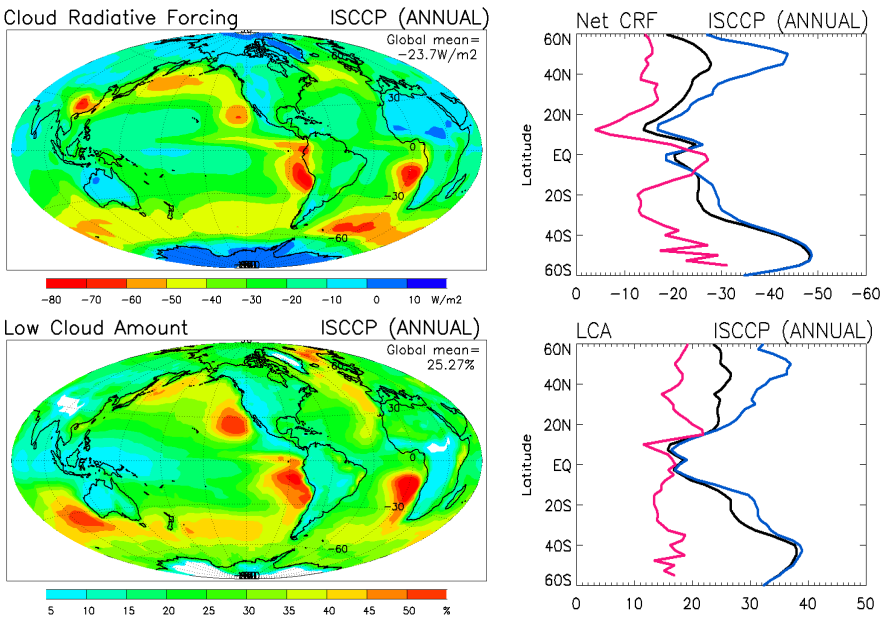

Figure 1 Horizontal distributions of net cloud radiative forcing (CRF, Wm^{-2}) and low-level cloud amount (LCA, %) from the ISCCP annual-mean climatology for the period of 1984-2007. Left panels are the zonal mean net CRF and LCA over ocean (blue), land (red) and total (black) area.

The ultimate goal of this research is to address cloud feedback in the future climate as predicted using current climate models. However, it is not yet certain whether the cloud feedback related to climate change is positive or negative. This is because current models exhibit a large range of global cloud feedbacks, with roughly half of the climate models predicting a more negative CRF in response to global warming, and half predicting the opposite (Soden and Held, 2006; Webb et al., 2006). Several studies show that inter-model differences in cloud feedbacks are mostly attributable to the SW cloud feedback component, and that the responses to global warming of both deep convective clouds and low-level clouds differ among GCMs (Bony and Dufresne, 2005; Webb et al., 2006; Wyant et al., 2006). Studies also suggest that the response of low-level clouds is the largest contributor to the range of climate

change cloud feedbacks among current climate models. The wide response range is due to the large discrepancies in the radiative response that are simulated by models in regions dominated by low-level cloud cover, which cover much of the globe. Figure 2 shows the CRF sensitivity to SST predicted by two groups of models in different regimes of the large-scale tropical circulation (the 500hPa vertical pressure velocity is used as a proxy for large-scale motions, with negative values corresponding to large-scale ascending motions, and positive values to sinking motions). The discrepancy between the two groups of models is greatest in regimes of large-scale subsidence. These regimes, which have a large statistical weight in the tropics, are primarily covered by low-level clouds. As a result, the spread of tropical cloud feedbacks among the models primarily arises from inter-model differences in the radiative response of low-level clouds in regimes of large-scale subsidence (Bony et al., 2006; Webb et al., 2006).

Since there are no observations available to verify cloud feedback in future climates predicted by current climate models, a practical method is needed to evaluate the model estimates. The most reliable practical method is to document the cloud variability associated with environmental factors observed in the current climate and evaluate the ability of climate models to simulate the sensitivity of low-level clouds (and CRF) to changes in environmental conditions. Several studies have sought to improve our understanding of the environmental controls operating on low-level clouds. These studies have shown that changes in local meteorological conditions can explain much of the variability in low-level cloud cover occurring on daily to interannual time scales (Klein and Hartmann, 1993; Norris and Leovy, 1994; Wood and Hartmann, 2006). Norris and Leovy (1994) found a negative correlation between SST and low-level cloud cover and noted the transition from stratiform to cumuliform clouds in regions with strong gradients of SST, with stratiform clouds most prevalent on the cool side of the gradients. Wyant et al. (1997) used a two-dimensional eddy-resolving model to study the equatorward transition from stratiform to cumuliform clouds. They found that rising SST acts to destabilize marine low-level clouds, eventually leading to the entrainment of dry air into the cloud deck and the replacement of stratus clouds with cumulus clouds.

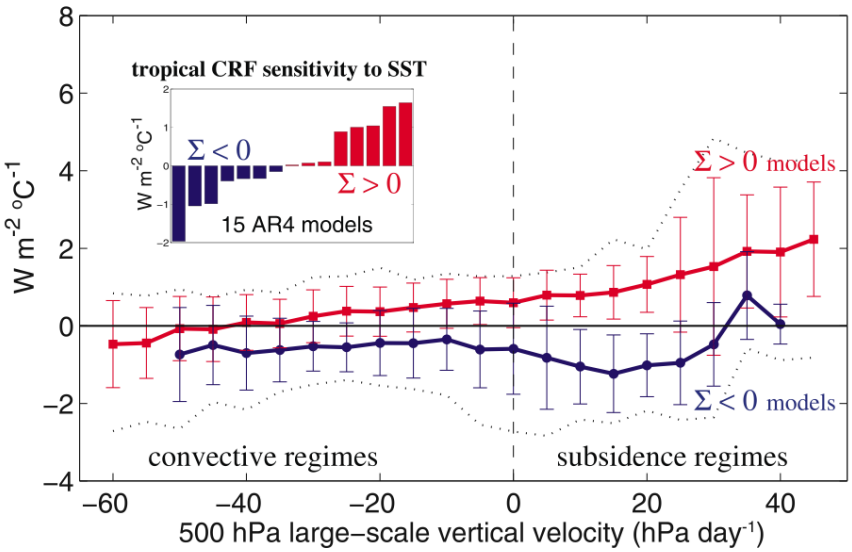

Figure 2 Sensitivity ($Wm^{-2}℃^{-1}$) of the tropical net cloud radiative forcing (CRF) to SST changes associated with global warming (simulations in which CO^2 increases by 1% yr^{-1}). Thick lines and vertical lines represent the mean and the standard deviation of model sensitivities within each group; dotted lines represent the minimum and maximum value of model sensitivities within each dynamical regime. The insert shows the tropically averaged climate change response of CRF to surface warming predicted by 15 AOGCMs used in the Fourth Assessment Report (AR4) of the Intergovernmental Panel on Climate Change. Adapted from Bony and Dufresne (2005).

Bony and Dufresne (2005) showed that a breakup of marine low-level cloud cover in regions of subsidence produces a strong positive feedback between the shortwave cloud radiative effect and SST. The influence of SST on low-level cloud cover may be by means of lower tropospheric stability (LTS), which correlates negatively with SST (Klein and Hartmann, 1993; Wood and Hartmann, 2006). They showed that higher low-level cloud fractions occurred under greater LTS. Clement et al. (2009) showed that lower LTS is coupled with higher SST in the NE Pacific and concluded that total cloud cover is reduced under warm SST. These studies have produced a consistent finding that reduced LTS can result from increased SST, which decreases cloud fraction by initiating the transition from stratiform to cumuliform cloud cover. Williams et al. (2006) found that by considering the CRF response to a change in large-scale vertical velocity and lower-tropospheric stability, a component of the local mean climate change cloud response can be related to present-day variability, and thus evaluated using observations. Stowasser and

Hamilton (2006) examined the ability of AOGCMs to simulate the change in tropical CRF due to SST change, in terms of large-scale vertical velocity and lower-tropospheric RH. They showed that the model results are most varied and least realistic in regions of subsidence, and to a lesser extent in regimes of deep convective activity.

Understanding the environmental controls on cloud cover and the evaluation of some components that control cloud feedback in current models should help to assess which of the model estimates of cloud feedback are most reliable. This study evaluates the low-level cloud variability produced by current climate models and tries to select the most reliable model for estimating cloud feedback. We will investigate interannual variations in observed and simulated climatologies of cloud amount and TOA radiative fluxes over the tropical ocean. The variability of low-level cloud amount in response to climate change and their relationships with possible driving factors such as atmospheric circulations and SST changes will be studied on local and global scales. Based on this study, the mechanisms responsible for these changes will be deduced.

2. METHODOLOGY AND DATA

In this study, we assume that the observed relationships between cloud cover and regional meteorological conditions provide a more complete way of testing the realism of cloud simulation in current-generation climate models. Based on such observations, we will select the most reliable model in terms of its performance in predicting low-level cloud cover (and CRF) and estimating low-cloud feedback in response to the warming climate. We examine cloud variations in observational cloud data and their relationships with meteorological variables to provide a physical framework for interpreting such variations. The information on total cloud amount, low-level cloud amount, and surface radiative fluxes was provided by the International Satellite Cloud Climatology Project (ISCCP). Other climate variables used in the analysis are sea surface temperature (SST) from the Hadley center reanalysis, and sea-level pressure (SLP), vertical velocity, surface winds, and lower tropospheric static stability

(potential temperature at 700mb minus surface temperature) from the ERA-40 reanalysis. Evaluations of low-level cloud feedbacks in the current climate and their changes in a warming climate are performed using simulations from 14 different coupled ocean-atmosphere models that have performed simulations in support of the Forth Assessment Report (AR4) of the Intergovernmental Panel on Climate Change (IPCC, Meehl et al., 2007).

2.1 Description of adjusted ISCCP data

The International Satellite Cloud Climatology Project (ISCCP) is an archive of cloud data retrieved from geostationary and polar-orbiting weather satellites. The ISCCP multi-decadal record of cloudiness exhibits a well-known global decrease in cloud amounts (Fig. 3). This downward trend has recently been used to suggest widespread increases in surface solar heating, decreases in planetary albedo, and deficiencies in global climate models. However, the trend showed by the ISCCP data has not been observed in surface (Norris, 2005) and other satellite (Jacobowitz et al., 2003; Wylie et al., 2005) cloud records. It has been suggested that the discrepancies between the ISCCP data and other observations may be the result of satellite artifacts in the ISCCP data, and that the downward trend is not related to physical changes in the atmosphere (Campbell, 2004; Norris, 2000).

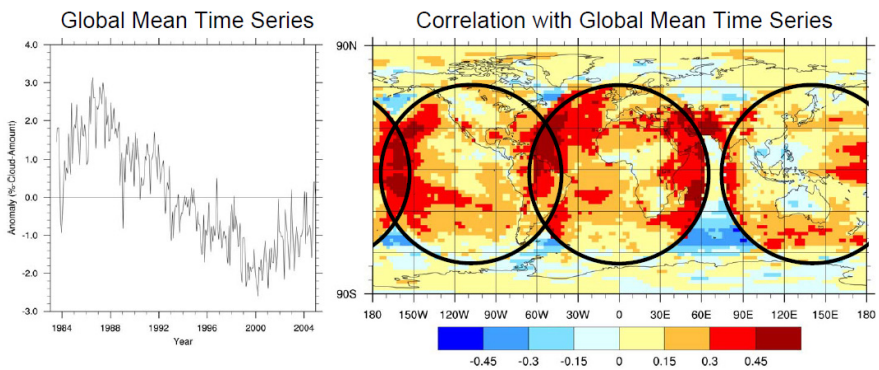

Figure 3 (left) Global mean time series of total cloud amount anomalies from original ISCCP IR data and (right) the correlation map of total cloud amount as a global mean time series.

Since the satellites used in ISCCP were not designed for climate monitoring, the nominal cloud record suffers from spurious variability associated with changes in instrumentation, shifts in orbit, and other problems. For example, systematic changes in satellite view angle cause artificial variations in retrieved cloud cover because clouds are more difficult to detect when closer to nadir due to a shorter optical path length through the cloud (Evan et al., 2007). Another problem is that the ISCCP satellite intercalibration process was imperfect, leading to similar changes in cloud cover across the entire view area of a satellite that was inconsistent with high-quality surface observations. To determine the regions that contribute the most to the decreasing trend of total cloud cover shown in Fig. 3, we display the correlation map of total cloud amount as a global mean time series. High correlation coefficients show a circular pattern centered in the Atlantic, Western Pacific and Eastern Pacific Oceans. These circles correspond to so-called geostationary "footprints" that describe the area observed by each satellite. Systematic changes in satellite view angle cause artificial variations in retrieved cloud cover.

To remove spurious long-term variability caused by satellite artifacts and retrieval errors, the procedure suggested by Clement et al. (2009) is applied before using the ISCCP data. At first, a spurious long-term variability caused by satellite artifacts is removed by linearly regressing out the portion of cloud variability associated with local changes in satellite view angle. Retrieval errors are removed by regressing out the time series of standardized cloud cover anomalies averaged over the entire view area of successive satellites from each individual grid box time series. This procedure removes all real cloud cover variability occurring on near-hemispheric spatial scales without impacting the regression patterns that focus on differences between regions. Clement et al. (2009) defined the resulting data as "adjusted ISCCP cloud cover". We used adjusted ISCCP cloud data using the D2 monthly mean cloud product for the years of 1984-2008 (Rossow and Schiffer, 1999), the most recent release. The ISCCP Flux Dataset was also constructed by applying a sophisticated radiative transfer model to ISCCP cloud data. The parameter used is the "cloud radiative effect", the change (from clear sky conditions) in downward radiation flux at the surface that results from the presence of clouds. We applied the two procedures described above to obtain the "adjusted ISCCP cloud radiative effect".

2.2 Description of model simulations

To evaluate whether AR4 models can reliably reproduce the observed variability of the cloud amount (and CRF) associated with meteorological variables, we use the monthly mean data of the twentieth-century coupled climate model simulations (20C3M) for the period of

Table 1 List of the 14 CGCMs used in this study and their configurations arranged in alphabetical order.

	CMIP3 designation	Institution	Resolution	
			Atmosphere	Ocean
1	CGCM3 T63 (CCCMa Coupled General Circulation Model version 3.1 T63 resolution)	Canadian Centre for Climate Modelling and Analysis (CCCMa), Canada	2.8125° ×~2.8125°	256×192
2	CNRM CM3	Meteo-France/Centre National de Recherches Meteorologiques, France	2.8125° ×~2.8125°	180×170
3	GFDL CM2_0 (Geophysical Fluid Dynamics Laboratory Climate Model version 2.0)	U.S. Department of Commerce/National Oceanic and Atmospheric Administration (NOAA)/GFDL, United States	2.5°×2.0°	360×200
4	GFDL CM2_1 (GFDL Climate Model version 2.1)	U.S. Department of Commerce/NOAA/GFDL, United States	2.5°×~2°	360×200
5	INM CM3 (Institute of Numerical Mathematics Coupled Model version 3.0)	Institute of Numerical Mathematics, Russia	5°×4°	144×84
6	IPSL CM4 (L'Institut Pierre-Simon Laplace Coupled Model, version 4)	Institute Pierre Simon Laplace, France	3.75°×~2.5°	180×170
7	MIROC3.2 HIG (MIROC3.2 high resolution version)	Center for Climate System Research (CCSR), National Institute for Environmental Studies (NIES), and Frontier Research Center for Global Change (FRGCG), Japan	1.40625° ×~1.40625°	320×395
8	MIROC3.2 MED (MIROC3.2 medium resolution version)	CCSR, NIES, and FRCGC, Japan	2.8125° ×~2.8125°	256×192
9	MPI ECHAM5 (ECHAM5/Max Planck Institute Ocean Model (MPI-OM)	Max Plank Institute for Meteorology, Germany	1.875° ×~1.875°	360×180
10	MRI CGCM2.3.2a	Meteorological Research Institute, Japan	2.8125° ×2.8125°	144×111
11	NCAR_CCSM3	National Center for Atmospheric Research, United States	1.40625° ×~1.40625°	320×395
12	NCAR_PCM1	National Center for Atmospheric Research, United States	2.8125° ×~2.8125°	360×180
13	UKMO HADCM3	Hadley Centre for Climate Prediction and Research, Meteorological Office, United Kingdom	3.75°×2.5°	288×144
14	UKMO HADGEM1	Hadley Centre for Climate Prediction and Research, Meteorological Office, United Kingdom	1.875°×~1.25°	360×216

1950-99. Table 1 presents a brief description of the 14 different coupled ocean-atmosphere models participating in the Forth Assessment Report (AR4) of the Intergovernmental Panel on Climate Change (IPCC, Meehl et al., 2007). The 20C3M simulations used late-nineteenth-century initial conditions and were executed to the end of the twentieth century, with historical anthropogenic and natural forcings. The external forcings resulting from atmospheric greenhouse gases and sulfate aerosols were prescribed across the simulations.

Feedback calculations are performed for climate change simulations integrated with projected increases in well-mixed greenhouse gases and aerosols as prescribed by the IPCC Special Report on Emissions Scenarios (SRES) A1B scenario. The data representing the future climate climatology span the period from 2050 to 2099. The future climate scenario roughly corresponds to a doubling in equivalent CO_2 between 2000 and 2100, after which time the radiative forcings are held constant. The estimated radiative forcing under this scenario is 4.3 Wm-2 (Ramaswamy et al., 2001). The uncertainty in forcings is estimated to be ~10% for the period of 1750-2000 and account for the uncertainty in the historical concentrations of the forcing agents.

3. OBSERVATIONAL GLOBAL CHARACTERISTICS OF CLOUDS

3.1 Spatial distribution and temporal variation of cloud cover

First of all, the characteristics of the climatological spatial distribution and the temporal variation of cloud cover are examined using adjusted ISCCP data. Figure 4 displays the geographical distributions of the annual mean total, low, and high cloud cover for the 288 monthly averages (1984-2007). The total cloud cover is primarily dominant over high-latitude Oceans, the eastern tropical Indian Ocean, the Intertropical Convergence Zone (ITCZ) near the Equator, and storm tracks in the mid-latitudes (as globally averaged to 67.2%). High-level cloud cover is evident near the equator and is associated with the location of the ITCZ, and also in the midlatitudes

where it is associated with cyclonic storm zones. These clouds are primarily composed of high clouds in the eastern tropical Indian Ocean and western Pacific, where deep convection takes place. On the other hand, low-level cloud cover is greatest over the subtropical eastern oceans in the midlatitudes and over the Arctic Ocean, and lowest over the western parts of the subtropical oceans where small trade wind cumuli are the predominant cloud type. Low-level clouds appear to be predominantly oceanic, where they represent 34% of total cloud cover, as opposed to 17.5% over land. The globally averaged low-level cloud amount is 25.3%. As shown in Fig. 1, the relationship between the climatological amounts of low-level cloud cover and the annual net cloud forcing is readily apparent, as regions with climatologically high amounts of low-level cloud cover are regions with strongly negative cloud forcing. In this study, we focused on the low clouds over the subtropical oceans and defined the subtropical marine low-level cloud regions as those where low-level clouds exceed 90% of total cloud cover.

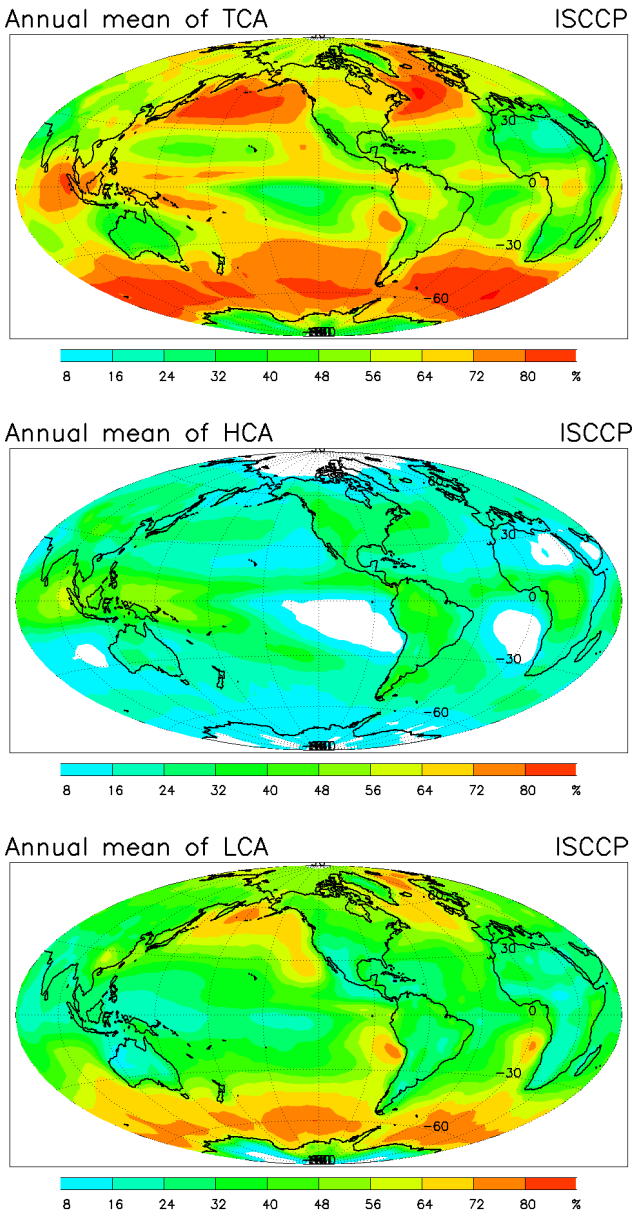

Figure 4 Global distributions of the annual mean total cloud, low-level cloud and high-level cloud amounts over ocean as derived from the ISCCP and averaged from January 1984 to December 2007.

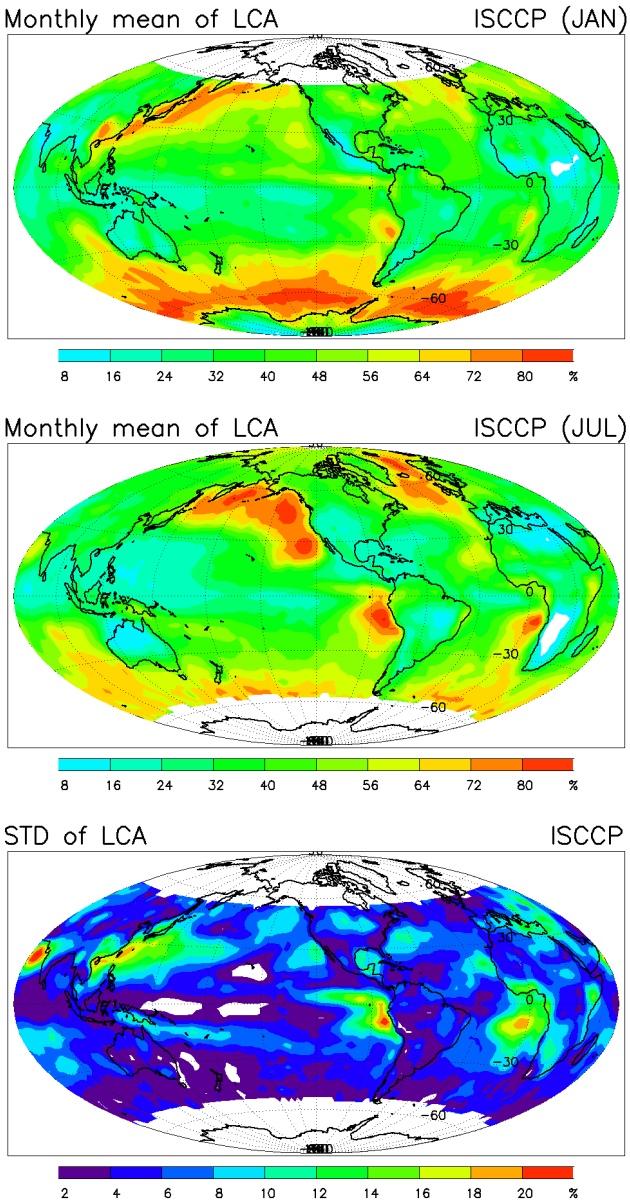

Figure 5 Global distributions of the monthly mean low-level cloud amounts for January and July, as well as their seasonal standard deviation (STD).

To assess the degree of seasonal variability, the standard deviations (STD) of monthly means of cloud amount are computed from the following equation:

$$\alpha = \sqrt{\frac{\sum_{n=1}^{N}(x_n - \bar{x})^2}{N-1}}$$

where α denotes the STD, N is 12(months), x represents the monthly mean fields of cloud amount, while $\bar{x}$ is the annual mean field of the cloud amount. Since a visible measurement to define the optical depth of cloud cover is required, it is necessary to determine where insolation falls below the level necessary for cloud measurement. Note that no data are available poleward of about 60° latitude in the winter hemisphere.

Figure 5 shows the seasonal character of the spatial distribution of low-level clouds. Seasonal variations in STD are evident and reflect the dominant seasonal time features. During January, low-level clouds show obvious maxima in the southeastern China Sea, the Circumpolar Ocean, and the storm track regions of the North Pacific and the North Atlantic. During July, low clouds greater than 60% are seen in the marine subtropical eastern oceans near the Californian, Peruvian, and Namibian regions, and in the Arctic and the North Atlantic, where sea surface temperature is comparatively low and where the mean air motion is downward. In the North Pacific, low-level clouds exceed 80% of total cloud cover. High-level cloud cover also changes seasonally, including southward (northward) shifts in January (July) (not shown). This pattern includes shifts over Africa, the southeast Asia/Maritime Continent monsoon complex, and South America. Over ocean, the seasonal shifts in high-level cloud cover are closely connected with intense tropical convection, such as over the equatorial western Pacific during January and the Bay of Bengal during July.

Table 2 The four low-level cloud regions, their geographical extents, and the seasons of maximum low-level cloud amounts.

Region	Location	Season of maximum low cloud
Californian	15-25N, 125-145W	JJA
Peruvian	15-25S, 80-90W	SON
Canarian	15-25N, 25-35W	JJA
Namibian	10-20S, 0-10E	SON

To more completely examine the seasonal characteristics of low-level clouds over the subtropical oceans, we display the seasonal variations of low-level cloud amounts averaged over the four subtropical marine regions in Table 2, where STD is shown (Fig. 6). A clear seasonal cycle is found in each of the regions, in general agreement with the findings of Klein and Hartmann (1993). Based on observations of stratocumulus clouds off the coast of California (Klein and Hartmann, 1993), it has been suggested that the summertime conditions under which stratocumulus clouds seem to occur include a well-developed subtropical high, equatorward-blowing trade winds whose divergence induces strong subsidence aloft, and a sharp temperature inversion at the top of a well-mixed layer. Low-level cloud amounts peak during JJA over the Californian and Canarian regions and during SON over the Peruvian and Namibian regions. For all of these regions, the seasonal cycle of low-level cloud amount is closely tied to the seasonal cycle of static stability, and indirectly related to the seasonal cycles of other parameters such as divergence or the strength of the subtropical high, as discussed in the following section.

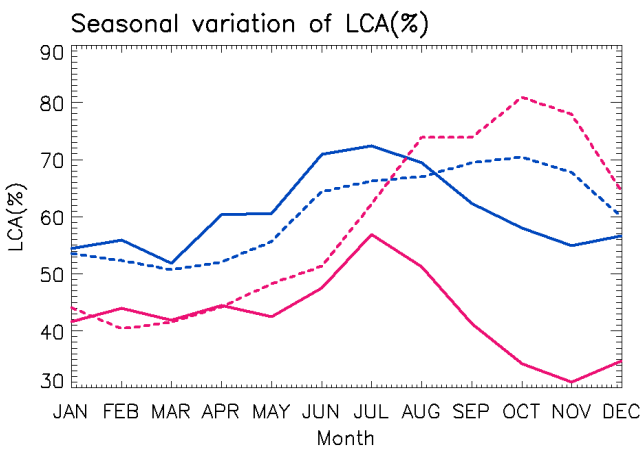

Figure 6 Annual cycles of low-level cloud amount (LCA) over the subtropical eastern oceans, such as the Californian (blue solid line), Peruvian (blue dotted line), Canarian (red solid line), and Namibian (red dotted line) regions.

3.2 Large-scale environment

In this chapter, we examine the environmental characteristics of the regions with persistent low-level clouds. Extensive low-level cloud cover is found with cold sea surface temperature and strong subsidence over tropical marine areas. Figure 7 shows the observed SST, vertical velocity at 500hPa, and the lower tropospheric static stability (LTS). The isolines of SSTs are generally parallel to the latitude, except for the west coastal region of the Americas and Africa where they are distributed along the coastline with the lowest SSTs near the coast. The small ocean-air temperature difference leads to climatologically weak surface fluxes of sensible heat. However, this alone could not be responsible for the maintenance of low-level clouds. In these regions, the strong cloud-top radiative cooling is the major component sustaining cloud cover. The lower tropospheric static stability (LTS) is considered to be a measure of the inversion strength (Klein and Hartmann, 1993), which is calculated as the difference between the potential temperatures at 700hPa and the surface. Large LTS is shown at the high latitudes with low sea surface temperature and in the subtropics within elevated inversion layers. LTS has been used in the parameterization of low-level cloud cover in general circulation models for the prediction of climate change (Larson et al., 1999). Strong, large-scale subsidence is also found in the same regions, which is related to the subsiding branches of the Hadley and Walker circulations. Klein and Hartmann (1993) showed that subtropical marine low-level clouds are generally most frequent in conditions of steady divergence with typical values of $2 \times 10^{-6} s^{-1}$

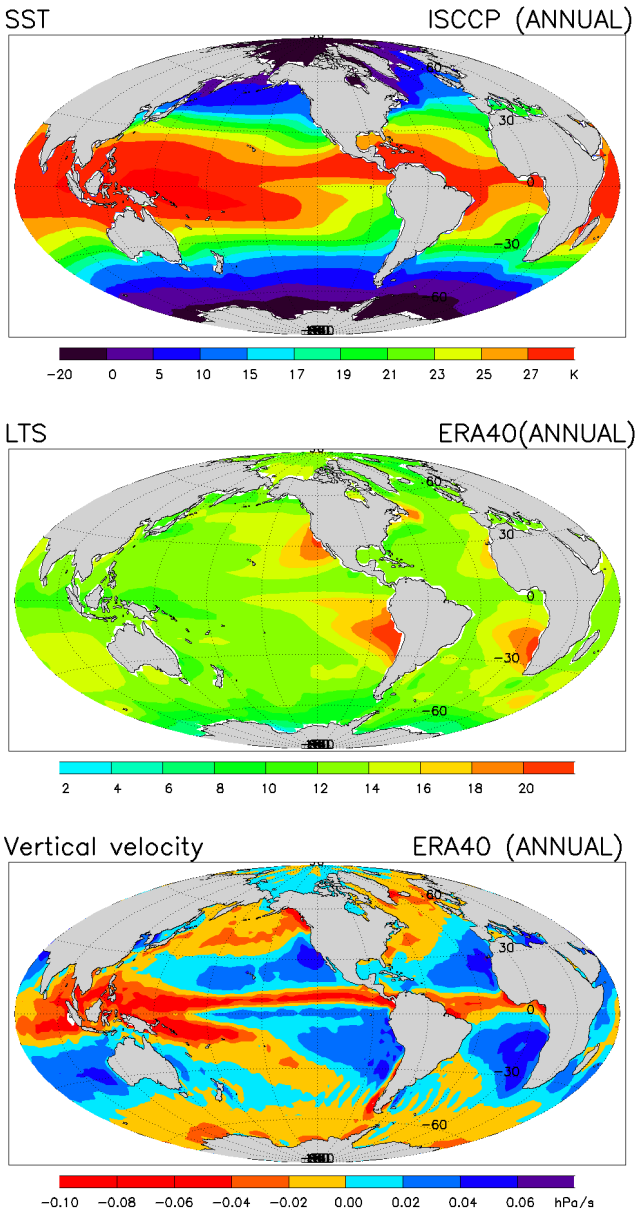

Figure 7 Global distributions of the observed SST, vertical velocity at 500hPa, and the lower tropospheric stability from ERA40 reanalysis data. The features are shown only over the ocean.

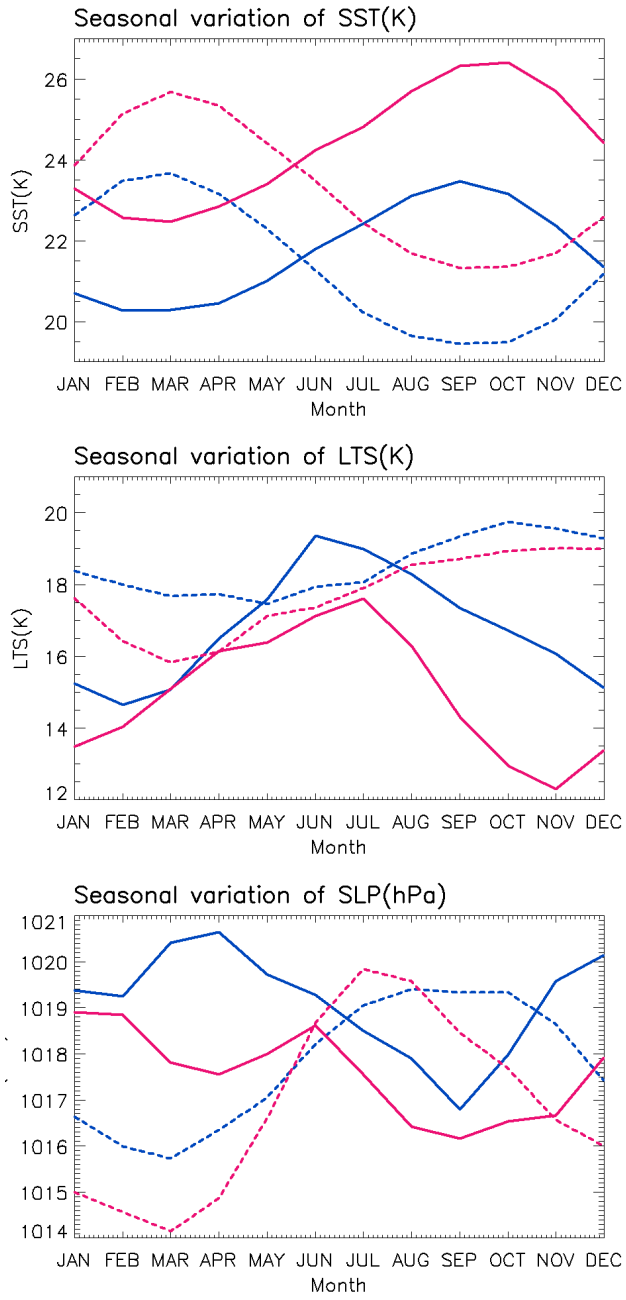

Figure 8 Annual cycles of sea surface temperature (SST), lower-tropospheric stability (LTS), and sea level pressure (SLP) over the subtropical eastern oceans, such as the Californian (blue solid line), Peruvian (blue dotted line), Canarian (red solid line), and Namibian (red dotted line) regions.

The seasonal variation of low-level cloud amount averaged over four subtropical marine areas in Table 2 is compared with the variation in thermodynamic parameters that could influence the occurrence of low-level clouds (Fig. 8). Over the Californian region, low-level cloud amount peaks at about 70% during July and reaches its minimum of about 52% in November (Fig. 6). This seasonal cycle corresponds to variation in lower atmospheric stability, LTS, indicating that the seasonal cycle of low-level cloud amount is closely tied to the seasonal cycle of stability. Note that the annual cycle in LTS is nearly identical to that of 700hPa temperature (not shown). Although the Canary Island region has a far lower low-level cloud cover, the seasonal cycle of low-level cloud amount in the Canarian region is similar to that of the Californian region, and lower amounts of low-level cloud cover are apparently associated with lower values of static stability. In contrast to the Californian region, the range of SST in the Southern Hemisphere low-level cloud region is greater than the range of 700hPa temperatures (not shown). Consequently, the static stability inversely follows the SST with maximum stability in October. The low-level cloud amount in this region peaks in the SON season, the season of maximum stability, at nearly 80%. The months during which the subtropical high reaches its peak sea level pressure are July and August, somewhat earlier than the months of maximum cloudiness. In the Namibian region, the peak low cloud amount occurs in October at nearly 70%, with the minimum occurs in February at 40%. These results indicate that the seasonal cycle of low cloud amount is closely tied to the seasonal cycle of static stability, and indirectly related to the seasonal cycles of other parameters such as divergence or the strength of the subtropical high.

3.3 Variations of low cloud cover correlated with meteorological variables

In order to show how meteorological variables influence cloud amount, we correlate cloud cover with variations in SST, as well as lower tropospheric stability (LTS), sea level pressure (SLP), and vertical velocity at 500hPa (W500). The correlations are calculated using the monthly mean anomalies relative to long-term monthly means. Each correlation is based upon 288 individual months of data (12 months per year over a 24-year span), meaning any correlation greater than ~0.2

in magnitude is significant at the 0.01 significance level.

Figure 9 shows the correlation between the local SST anomaly and the cloud amount anomalies, including those of total, low-level and high-level cloud cover. The three maps show that each individual cloud amount anomaly is differently correlated with SST. Overall, low-level clouds are negatively correlated with SST, except for a weak positive correlation over the central Pacific. Especially, there is strong signal over the subtropical marine areas and along the Equator in the Pacific. This negative correlation is consistent with that shown by previous observational studies (Norris and Leovy, 1994; Wyant et al., 1997; Clement et al., 2009). On the other hand, high-level clouds show positive correlation with SST in the equatorial Pacific, but little correlation elsewhere. Note that low-level clouds are negatively correlated with SST, while high-level clouds are positively correlated with SST. This implies the transition from low-level to high-level clouds. These results support that the rising SST acts to destabilize the boundary layer and eventually lead to the entrainment of dry air into the cloud deck and replacement of low-level clouds with high-level clouds (Wyant et al. 1997). The pattern of correlations shown for total cloud cover faithfully reflects the properties of both high- and low-level clouds, i.e., the negative correlation in the regions of persistent marine low-level cloud cover and the positive correlation of high-level cloud cover in the equatorial Pacific. Because the clouds over subtropical marine areas are mainly composed of low-level clouds (Fig. 10), the properties of the total cloud cover reflect those of low-level clouds, especially their being negatively correlated with SST. Note that the subtropical marine low-level cloud regions are defined as the regions where low-level clouds exceed 90% of total clouds.

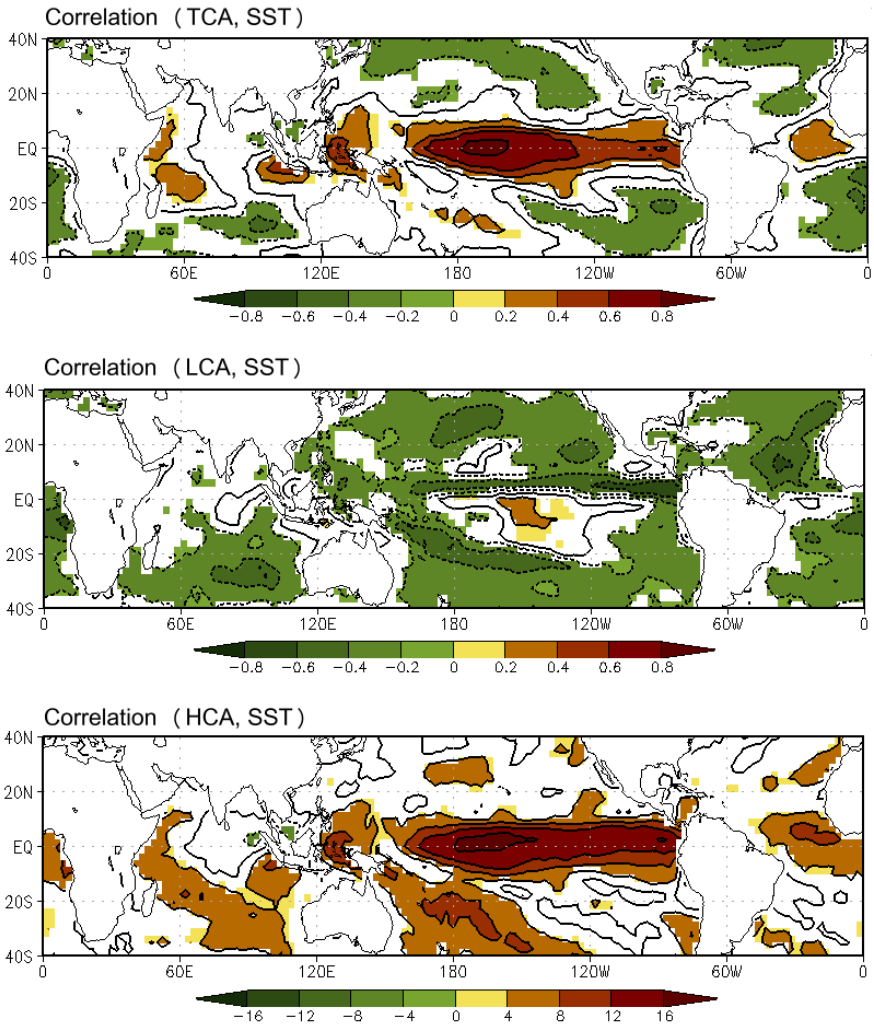

Figure 9 Correlation between SST (UK Met Office HadISST1) and (upper) total cloud cover, (middle) low cloud cover, and (bottom) high cloud cover. Correlations are shown as contour, which solid lines representing positive correlations and dotted lines representing negative correlations. Cloud amount and SST anomalies are monthly anomalies relative to long-term monthly means. The shaded areas are significant at the 0.01 significance level.

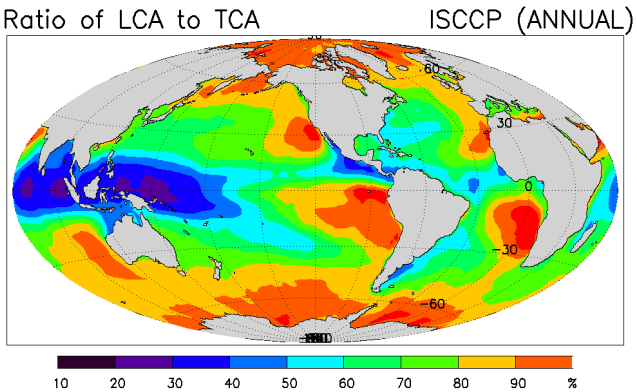

Figure 10 Ratio of low-level cloud amount to total cloud amount. Marine low-level cloud regions where low-level clouds exceed 90% of total clouds are shaded by orange and red colors.

The climatological distribution of low-level clouds closely matches that of stability (Fig. 4 and Fig. 7), and anomalies in low-level cloud amount are better related to anomalies in stability than anomalies in surface temperature (Klein and Hartmann, 1993). Figure 11 shows the relationship between LTS and low-level and total cloud amounts. In the subtropical marine low-level cloud regions showing a negative correlation between SST and low-level cloud amount, LTS consistently has the strongest relationship with variations in low-level cloud amount. Although SST is negatively correlated with low-level cloud amount at the 99% confidence level, LTS is positively correlated with low-level cloud amount. Reductions in LTS can be caused by increasing SST, which causes a decrease in cloud fraction by initiating a transition from low-level to high-level clouds. Thus, as expected, the correlation between high-level cloud amount and LTS shows an opposite sign compared to that between low-level cloud amount and LTS (not shown). Therefore, the pattern of correlation for total cloud amount is positive in the regions of persistent marine low-level cloud cover and the negative over the equatorial Pacific.

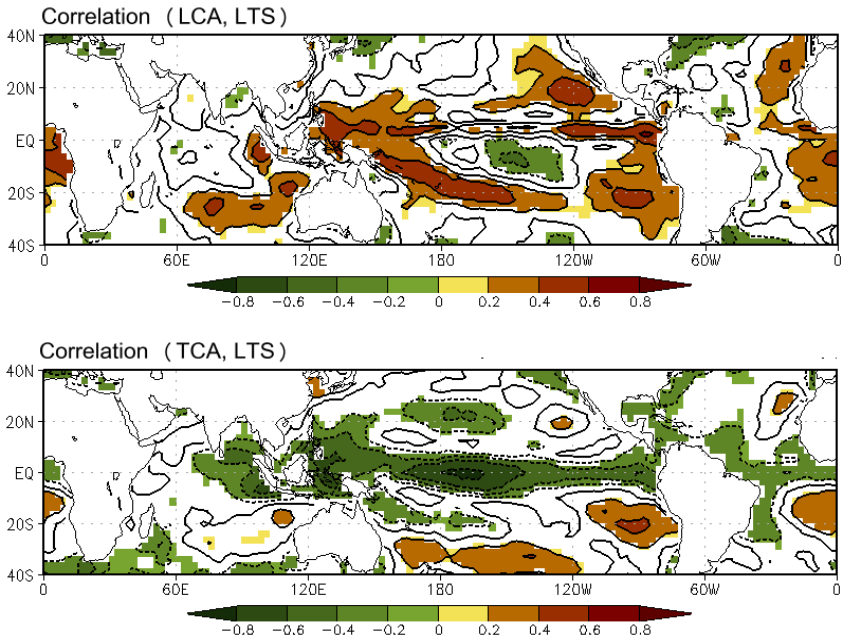

Figure 11 Correlation between LTS and (upper) low-level cloud amount and (bottom) total cloud amount. Correlations are shown as contours, of which the solid and dotted lines represent positive and negative correlations, respectively. Cloud amount and SST anomalies are monthly anomalies relative to long-term monthly means. The shaded areas indicate significance at the 99% level.

Aside from SST and LTS (connected to the atmospheric thermal structure), other factors (related to large-scale circulation) also play a role in the variation of low-level clouds. George and Wood (2010) show that changing SLP, associated with changing circulation, plays a role in modulating low-level cloud cover. To examine the relationship between large-scale circulation and low-level cloud cover, we also correlate cloud cover with SLP and vertical velocity. Figures 12 and 13 show the correlations between the local SLP and vertical velocity anomalies and the cloud amount anomaly, respectively. Over subtropical marine areas, low-level clouds are positively correlated with SLP, and the degree of correlation should give a measure of the strength of subsidence. This means that high pressure by subsidence is one of the drivers of variation in low-level cloud amount. We examined other variables such as RH and surface wind speed, but they showed little correlation with low-level cloud amount.

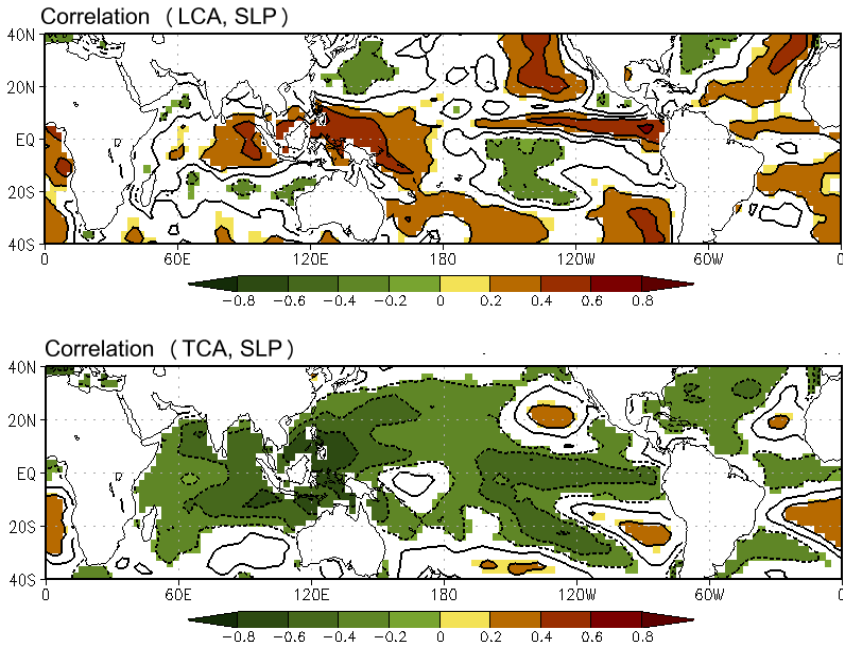

Figure 12 Same as Fig. 11 except for sea level pressure.

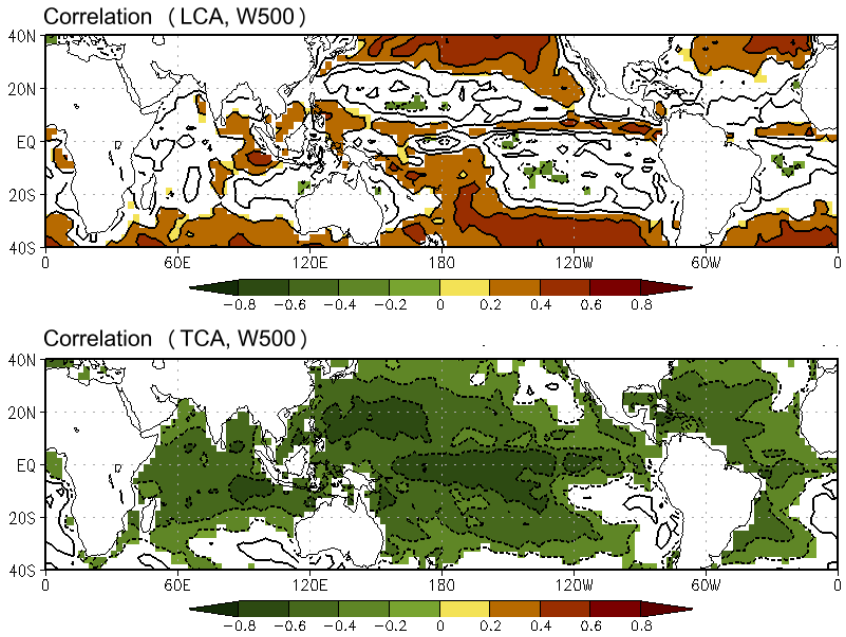

Figure 13 Same as Fig. 11 except for vertical pressure velocity (hPa/ s) at 500hPa.

In regions of persistent low-level cloud cover (tropical marine areas), the correlations of low-level cloud cover anomaly with a variety of meteorological variables suggest that low-level clouds are associated with the cool sea surface temperatures, stronger stability, higher sea level pressure, and subsidence of tropical marine regions. These results support a mechanism hypothesized by Wyant et al. (1997), in which an increase in SST causes a reduction in lower tropospheric stability that allows for more vertical motion within and around the cloud deck and leads to an increase in dry air entrainment. This brings about a reduction in cloudiness and a transition from low-level to high-level cloud types. Higher SLP could also produce more subsidence aloft, thereby increasing LTS independent of SST.

4. EVALUATION OF MODEL SIMULATIONS

4.1 Model evaluation for the simulated cloud variations

To examine whether AR4 models can reliably replicate the observed variations in low-level cloud amount associated with meteorological variables, we analyze the 20^{th} century climate simulation of 14 CGCMs (Table 1). The correlations are based upon 600 individual months of data (12 months per year over a 50 year span) and calculated using monthly anomalies relative to long-term monthly means of the meteorological variables. For the evaluation of simulated low-level cloud variations, we use total cloud cover instead of low-level cloud cover because the separate low-level cloud cover is not made available in the archive of most of the CGCMs. In addition, total cloud cover well represents the characteristics of low-level cloud cover over the persistent low-level cloud regions (subtropical marine areas) that are the focus of study.

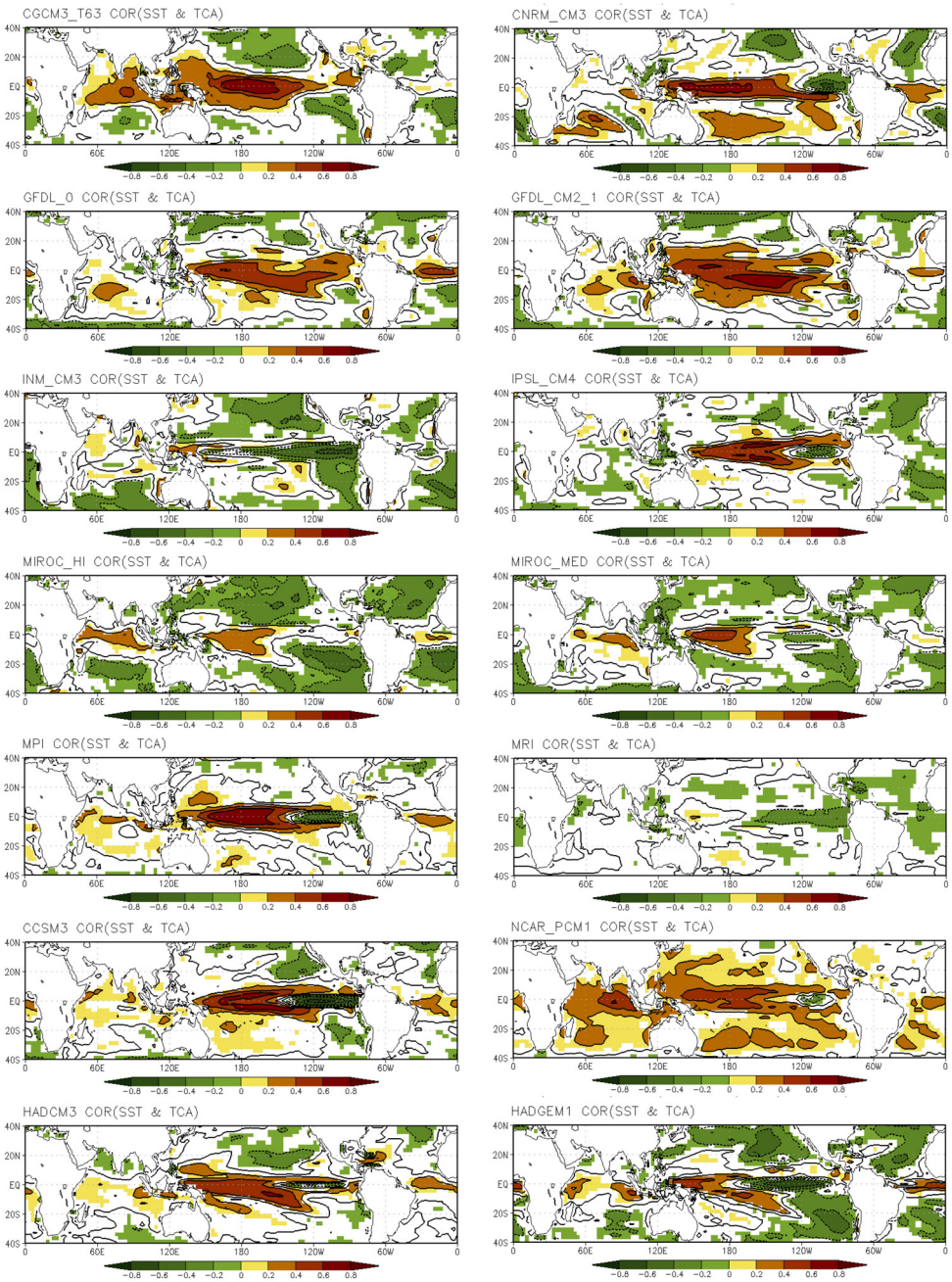

Figure 14 Comparison of correlations between total cloud amount (TCA) and SST anomalies obtained from 14 OCGMs. Correlations are shown as contours and the anomalies are monthly anomalies relative to long-term monthly means. The shaded areas indicate significance at the 99% level.

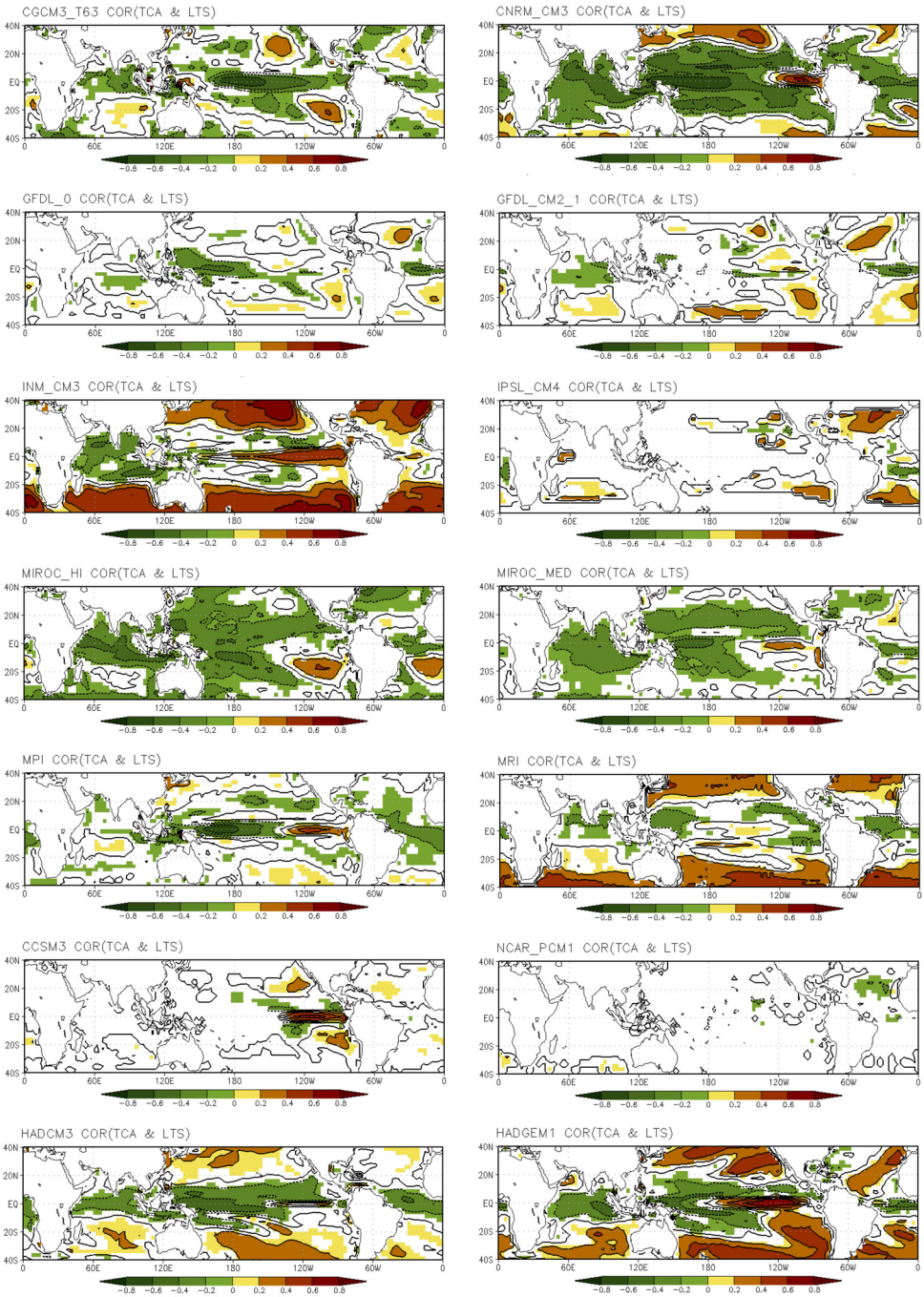

Figure 15 Same as Fig. 14 except for lower-tropospheric stability (LTS).

For the SST, the observed total cloud cover shows a negative correlation over the subtropical marine areas with persistent low-level cloud cover and a positive correlation over the equatorial Pacific with strong convection activity (Fig. 9). Figure 14 displays the correlations computed using the modeled total cloud amount (TCA) and sea surface temperature (SST) anomalies. The observed spatial pattern is reproduced fairly well in several models, especially in CGCM3, GFDL_0, GFDL_1, IPSL_CM4, and HACD3. The strength and spatial extent of the positive and negative correlations are best represented by the CGCM3 compared to observations, with maximum positive correlations of -0.6 ~-0.8 in the equatorial central Pacific and negative correlations of 0.2 ~ 0.4 over the subtropical marine areas. However, many models are unable to capture this spatial pattern of observed correlation coefficients. In INM_CM3, MIROC_HI, MIROC_MED, and HADGEM1, the subtropical negative correlations are too strong and extend too far in the equatorward direction. Even INM_CM3, HADGEM1 and CCSM3 show strong negative correlations over the equatorial eastern Pacific, which are opposite the signs of the correlation coefficients of the observations. The other models have positive correlations over the subtropical marine areas or show spatial patterns of correlation coefficients that have indistinct areas of statistical significance.

Observations show that LTS also maintains a consistent relationship with cloud amount, including positive correlation over the subtropical marine areas and negative correlation over the equatorial Pacific (Fig. 11). That is, LTS maintains a similar spatial pattern to that seen between SST and cloud amount, although with an opposite sign (Fig. 9). Few models can capture the observed spatial pattern of the correlation between TCA and LTS (Fig. 15). Especially, the strength and spatial extent of the observed spatial pattern are well represented by the CGCM3, with maximum negative correlations of -0.6 ~-0.8 in the equatorial central Pacific and positive correlations of 0.2 ~ 0.4 over the subtropical marine areas. Although the GFDL_0 and the HADCM3 generate this general spatial pattern, their strengths of correlation over the subtropical eastern ocean is weaker than the observed pattern. The INM_CM3 and HADGEM1 show an overly strong positive correlation in all subtropical ocean areas and the equatorial eastern Pacific, while the CNRM_CM3 and the MIROC_MED give an overly strong negative correlation in all tropical regions. In case of MIROC_HI, GFDL_1,

IPSL_CM4, and CCSM3, the positive correlations over subtropical eastern ocean areas are fairly well matched to the observed pattern, but the models give negative correlations over the tropical oceans that are overly weak or excessively extended to higher latitudes compared to observations. The other models, the MPI, MRI, and NCAR_PCM, give negative correlations (opposite sign compared to observed patterns of correlation) over the subtropical eastern oceans or show indistinct areas of statistical significance.

Aside from SST and LTS, other factors related to large-scale circulation certainly play a role in the variation of cloud amount (Fig. 12, Fig. 13). In Fig. 16 and Fig. 17, we display the modeled relationships between total cloud amount and SLP, and vertical velocity. The observed total cloud amount correlated with SLP shows a negative correlation throughout the tropical and subtropical ocean areas, with a maximum negative correlation coefficient of about -0.6 in the western Pacific Ocean, while significant positive correlations are shown over the subtropical eastern marine areas. Only two models, the CGCM3 and the HADGEM1 reproduce this observed spatial pattern. Most models can't capture the positive correlation of low-level cloud amount with SLP. The IPSL_CM4, CCSM3, and NCAR_PCM1 models do not show distinct areas of statistical significance. Regarding vertical velocity, all of the models except CCSM3 show a negative correlation with total cloud amount over all ocean areas, while only two models, the CGCM3 and MIROC_HI, reproduce the positive correlation observed over the subtropical low-level cloud regions. Note that actual numerical values of correlations are less meaningful because these variables are not independent. Instead, patterns that are broadly consistent across different regions are considered to be better indicators of significance.

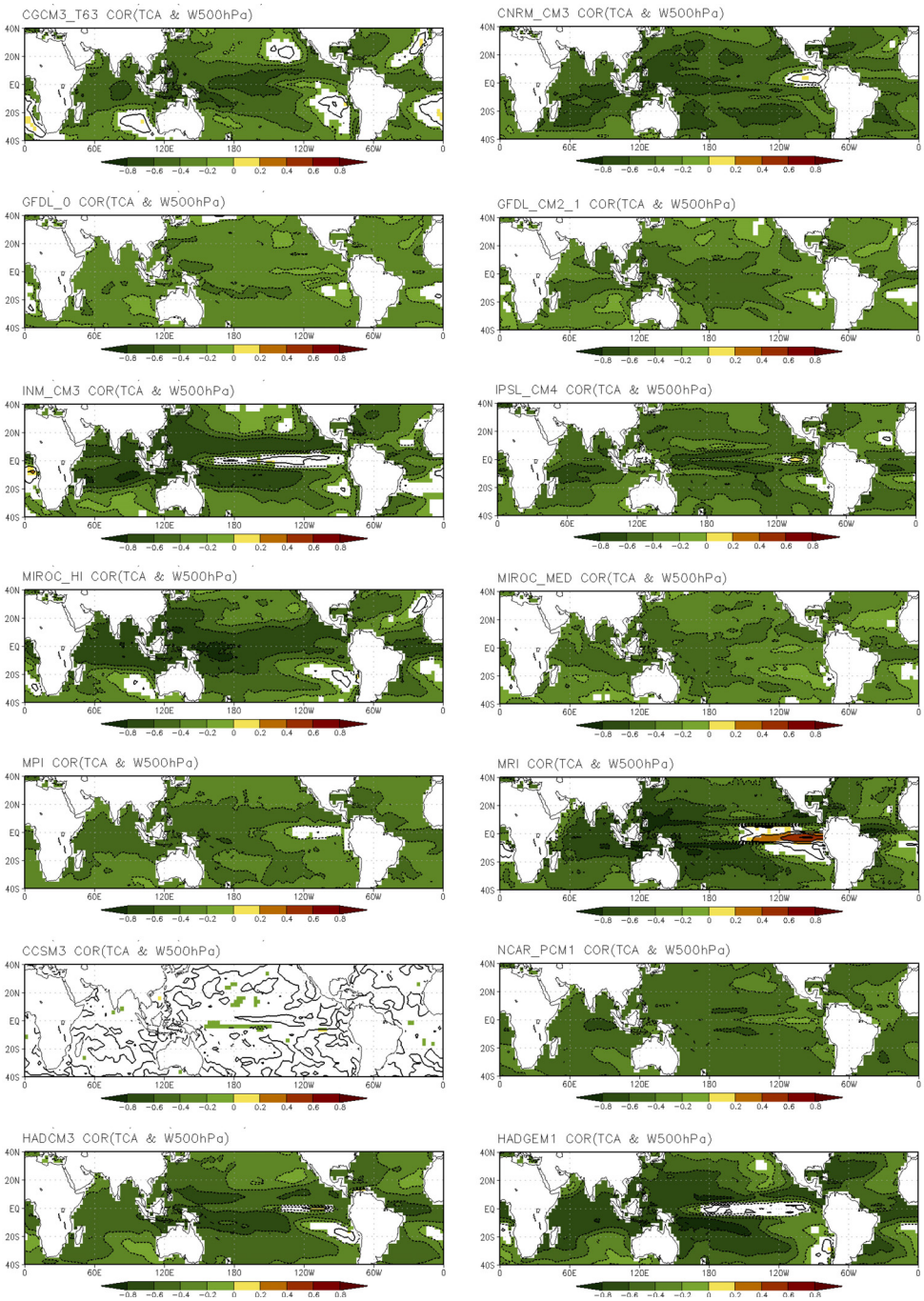

Figure 17 Same as Fig. 14 except for pressure vertical velocity anomalies at 500hPa (W500).

The spatial patterns of relationships between cloud amount and meteorological variables are summarized by computing pattern correlations. The pattern correlations of total cloud anomalies correlated with the local thermal structure (SST, LTS) and circulation (SLP, W500) are computed for each model (Fig. 18). Each coefficient is averaged over the ocean areas within 40°S~40°N in latitude and 0°E~360°E in longitude. Most models poorly reproduce the general response of cloud amount to changes in meteorological variables. Only three models show pattern correlation coefficients over 0.4 for all variables; the CGCM3, GFDL_0, and HADCM3. In Figs. 14-17, the CGCM3 well reproduces the observed spatial pattern of cloud response to the change in all variables, including the contrast response over the tropical Pacific and subtropical eastern oceans. While the GFDL_0 and the HADCM3 have similar values for all variables, they fail to capture the contrast structure over tropical ocean areas and the subtropical eastern oceans. Because the evidence of low-level cloud cover in the cloud-meteorology correlation test only occurs in confined regions, the pattern correlation is not sufficient to determine whether the model shows correlation that is consistent with the observed pattern. Therefore, evidence of low-level cloud responses must be examined in greater detail.

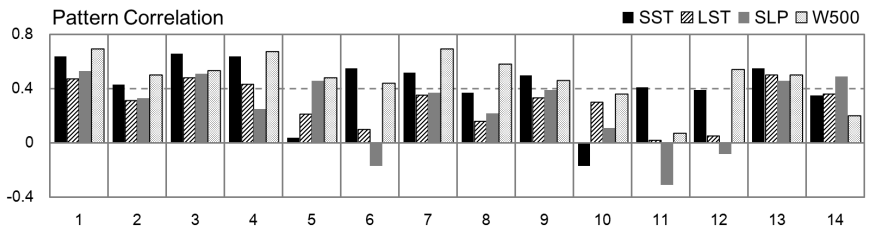

Figure 18 Pattern correlation coefficients of correlation between total cloud amount and various meteorological variables for observations and climate models. Each coefficient is averaged over the ocean within 40S-40N in latitude and 0-360 in longitude. Each number corresponds to a particular GCM (see Table. 1). 1: CGCM3, 2: CNRM, 3: GFDL_0, 4: GFDL_1, 5: INM_CM3, 6: IPSL, 7: MIROC_HI, 8: MIROC_HI, 9: MPI, 10: MRI, 11: CCSM3, 12: NCAR_PCM, 13: HADCM3, 14: HADGEM1

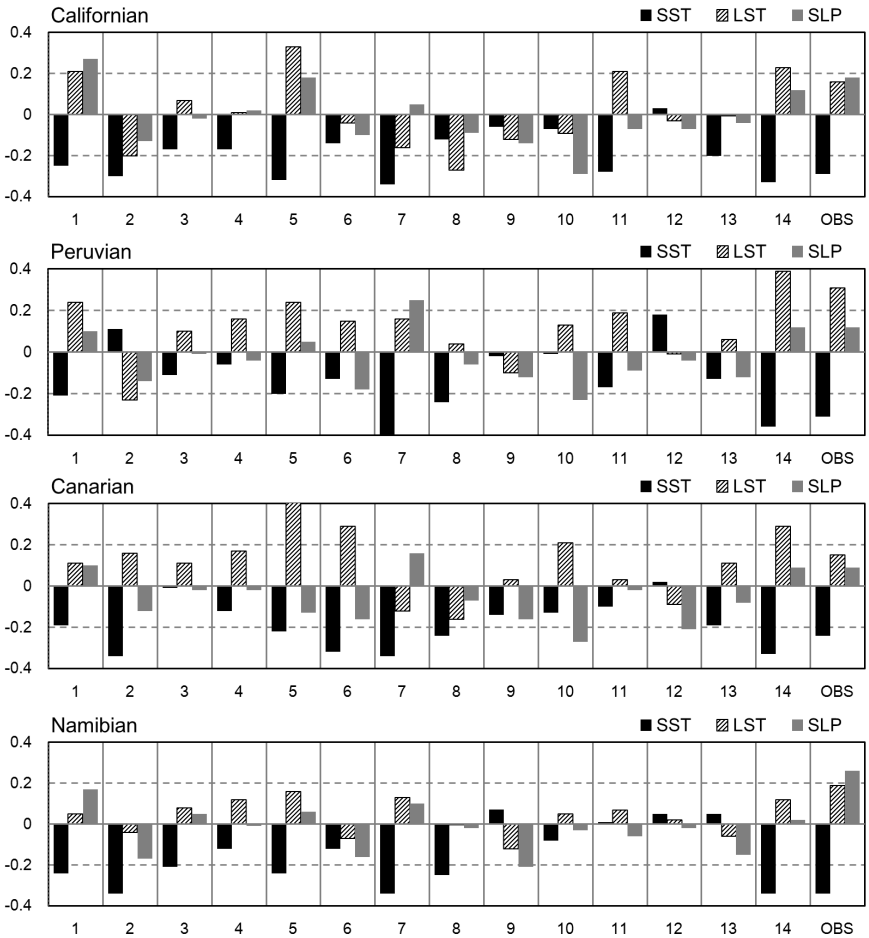

Figure 19 Correlation between cloud amount and various meteorological variables in four marine areas for observations and climate models. Each number corresponds to a particular AOGCM (see Table. 1). The selected areas are indicated Table 2. For the comparison, the total cloud amounts are correlated with observed SST (black bar), lower tropospheric stability (LTS, slashed bar), sea level pressure (SLP, gray bar), and mid-tropospheric pressure vertical velocity (W500).

The correlations between cloud cover and meteorological variables in low-level cloud regions are computed for each model and compared with observations in Fig. 19. In this study, we define the low-level cloud region as the region where low-level clouds exceed 90% of total clouds. The coefficients are averaged over each area (indicated in Table 2). Over the defined regions, specifically the Californian, Peruvian, Canarian, and Namibian, the observed correlations of low-level cloud cover with

meteorological variables show consistent sign, specifically negative correlations for SST and positive correlations for LTS and SLP. Here, SLP is selected as a simple measure of the response of low-level cloud cover to changes in climate dynamics, specifically as a measure of subsidence strength. The positive correlation between low-level cloud amount and SLP indicates that low-level cloud cover increases when there is anomalously positive stability induced by decreased SST under stronger subsidence conditions. Models are selected according to whether their correlations are of the correct signs relative to observations. By successively eliminating models on this basis, we are left with only two that correctly simulate the correlations for all variables; the CGCM3 and the HADGEM1.

define the low-level cloud region as the region where low-level clouds exceed 90% of total clouds. The coefficients are averaged over each area (indicated in Table 2). Over the defined regions, specifically the Californian, Peruvian, Canarian, and Namibian, the observed correlations of low-level cloud cover with meteorological variables show consistent sign, specifically negative correlations for SST and positive correlations for LTS and SLP. Here, SLP is selected as a simple measure of the response of low-level cloud cover to changes in climate dynamics, specifically as a measure of subsidence strength. The positive correlation between low-level cloud amount and SLP indicates that low-level cloud cover increases when there is anomalously positive stability induced by decreased SST under stronger subsidence conditions. Models are selected according to whether their correlations are of the correct signs relative to observations. By successively eliminating models on this basis, we are left with only two that correctly simulate the correlations for all variables; the CGCM3 and the HADGEM1.

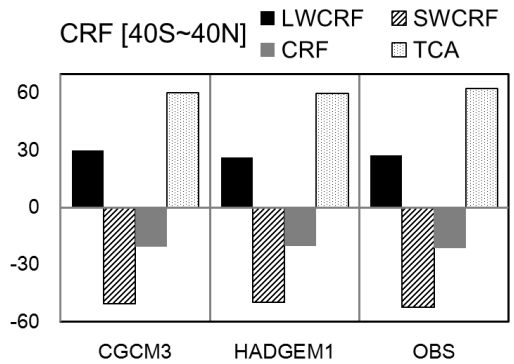

Figure 20 Comparison of longwave, shortwave and net cloud forcing, and total cloud amount from ISCCP fluxes with estimates from two GCMs, the CGCM3 and the HADGEM1. Net radiative forcing is indicated as the sum of LWCRF and SWCRF. Each value is averaged over the ocean within 40S-40N in latitude and 0E-360E in longitude.

We compare the cloud radiative forcings simulated by the selected two models with observed forcing (Fig. 20). Each value is averaged over the ocean within 40°S~40°N in latitude and 0°E~360°E in longitude. The observed net radiative forcing indicates that the net effect of clouds is to cool the ocean. The total cloud amount is observed to be about 62.4%, and net cloud forcing is -21.4Wm^{-2}. This net cooling is obtained from a longwave cloud-radiative warming of 27.4Wm^{-2} and a shortwave cooling of -52.2Wm^{-2}. Two models, the CGCM3 and the HADGEM1, exhibit considerably good agreement with observed net cloud radiative forcing, including with the cooling and warming effects of shortwave and longwave radiation, suggesting that the models can reliably model the performance of cloud radiative forcing and low-level cloud amount.

4.2 Change of cloud amount (and CRF) by global warming

We evaluate how cloud feedback would operate in a global warming climate due to increased greenhouse gases. We estimate low-level cloud feedback in a global warming climate using the selected models, the CGCM3 and the HADGEM1. Feedback calculations are performed for climate change simulations integrated with projected increases in well-mixed greenhouse gases and aerosols as prescribed by the IPCC Special Report on Emissions Scenarios (SRES) A1B scenario. The data span the period

from 2050 to 2099. (This A1B scenario corresponds roughly to a doubling in equivalent CO2 between 2000 and 2100, after which time the radiative forcings are held constant. The estimated radiative forcing under this scenario is 4.3 Wm-2 (Ramaswamy et al., 2001). The uncertainty in forcings is estimated to be ~10% for the period of 1750-2000, which includes uncertainty in the historical concentrations of the forcing agents themselves.) Note that the 'Change' (hereafter) is defined as the annual mean for the period of 2050-2099 from the A1B scenario minus the annual mean for the period of 1950-1999 from the 20C3M simulations.

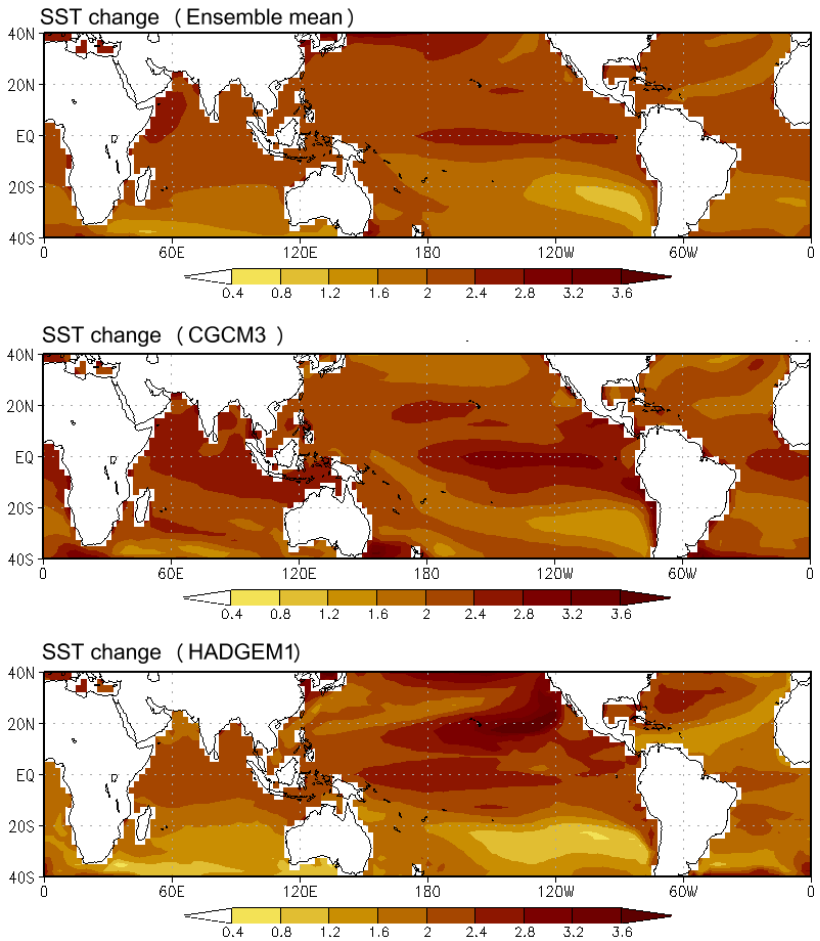

Figure 21 Changes in sea surface temperature (SST) for ensemble mean of 14 CGCMs, and the best models, the CGCM3, and the HADGEM1.

Figure 21 shows the annual mean change in SST associated with the increased greenhouse gases. SST change is positive in all locations, but the spatial variance of the variable differs between the models. For the ensemble mean of the 14 CGCMs, SST change is less than 2K and weaker south of the equator, particularly off the west coast of South America. The ensemble mean of SST shows limited spatial variance, while the spatial variance of each model is quite large in the tropics and subtropics. The CGCM3 and the HadGEM1 show higher amplitudes of SST warming than the ensemble projections and also show different maximum changes in SST. The CGCM3 shows a local maximum of SST change off the west coast of North America, while the maximum SST change is shown by the HadGEM1 model in the equatorial eastern Pacific. The differences between the spatial patterns of SST change in both models might be partially reflective of the feedback between their different cloud responses to the global warming.

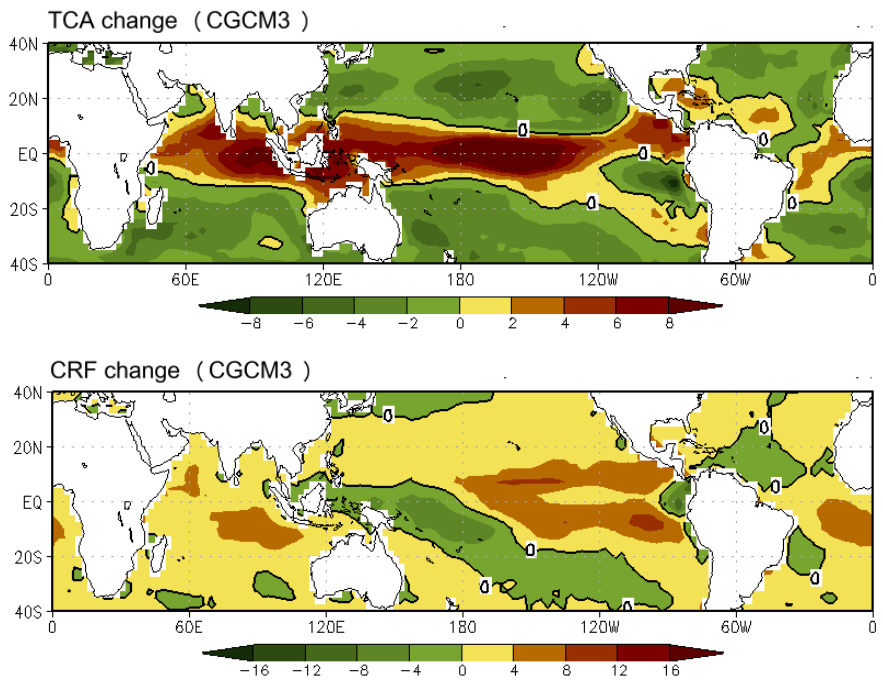

Figure 22 Changes in total cloud amount (TCA) and cloud radiative forcing (CRF) for the CGCM3.

Figures 22 and 23 show the spatial patterns of changes in cloud cover and radiative forcing, which are largely comparable to that of SST in Fig. 21. In the CGCM3 (Fig. 22), total cloud change shows a relatively symmetrical structure, with maximum increase over the equatorial Pacific and Indian Oceans and a decrease over all subtropical oceans including the marine low-level cloud regions. On the other hand, the maximum increase in cloud radiative forcing is shown over the western Pacific Ocean and a decrease is shown over the western Pacific Ocean. The different spatial distributions of change might be induced by the different responses of various cloud types to the global warming climate. Note that low-level clouds dominate the shortwave cooling effect, while high-level clouds dominate the longwave warming effect on the climate. Over the subtropical eastern ocean areas, it is evident that SST warming can induce a reduction in the low-level cloud amount and lead to a positive CRF. The increased total cloud cover over the equatorial western Pacific can be understood as an increase in the high-level cloud amount or a transition from low-level to high-level clouds.

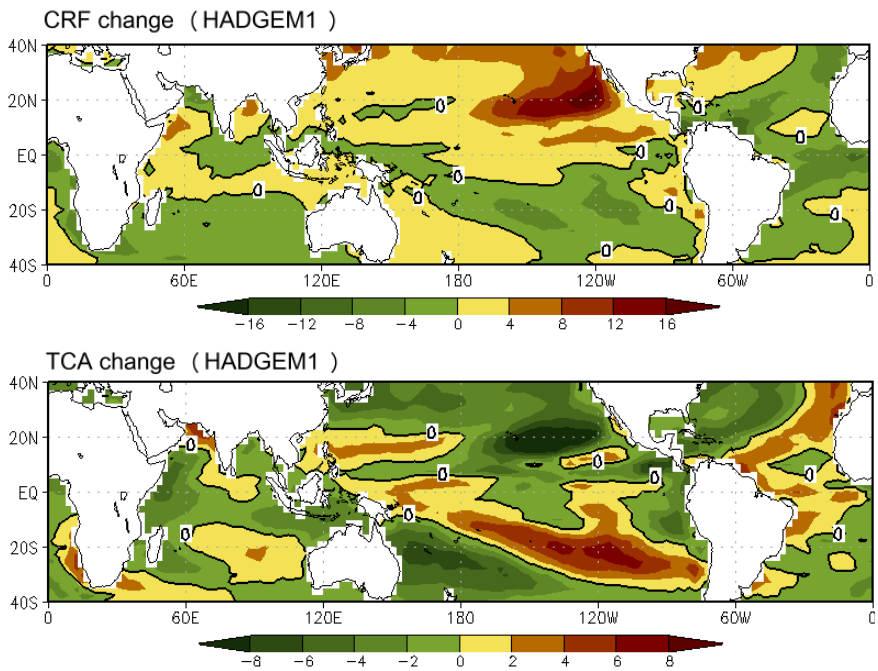

Figure 23 Changes in total cloud amount (TCA) and cloud radiative forcing (CRF) for the HADGEM1.

In the HADGEM1 (Fig. 23), the change in total cloud cover brings a corresponding change in cloud radiative forcing. The reduced (increased) cloud cover occurs off the west coast of North (South) America with the local maximum (minimum) of SST change, which causes positive (negative) cloud radiative forcing. This result is mainly caused by the shortwave cooling effect of the low-level clouds. Although we cannot evaluate the exact causes of these cloud changes without additional experiments, the decreased cloud cover in subtropical stratocumulus regions appears to result from warmer SST and a weakening of the large-scale atmospheric circulation in the Pacific in both models (not shown).

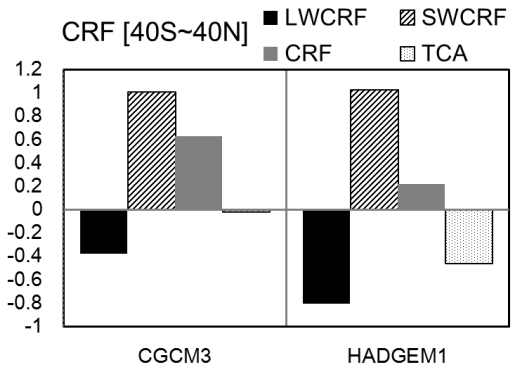

Figure 24 Changes in the cloud radiative forcing in the longwave (LWCRF), shortwave (SWCRF), net radiative forcing, and total cloud amount. The actual values are divided by the surface temperature increases, which are different among the models, to have the unit of $Wm^{-2}K^{-1}$ for the fluxes and % K^{-1} for the cloud amount. Each value is averaged over the ocean within 40S-40N in latitude and 0-360 in longitude.

Finally, we summarize the cloud feedback in the future climate using the reliable model which is selected based on the cloud-meteorology correlation test. Figure 24 shows the changes in the cloud radiative forcings for the best two models, the CGCM3 and HADGEM1. Each value is divided by the increase in surface temperature to indicate how much the cloud contributes to the amplification or moderation of direct radiative forcing in the future climate. Both models exhibit relatively good agreement with the projected changes in cloud forcing, with negative and positive signs for longwave and shortwave radiation, respectively, as total cloud cover is shown by both models to decrease in a globally warming climate. The figure also shows the changes in

global mean total cloud amounts attributable to the different cloud types. Although the CGCM3 shows less of a reduction in cloud cover than the HADGEM1, it shows stronger positive cloud forcing due to the reduction of low-level cloud cover over subtropical ocean areas.

5. SUMMARY

In this study, we investigate interannual variations in observed and simulated climatologies of cloud amount and TOA radiative fluxes over the tropical ocean. The variations of low-level cloud amount in response to climate change and their relationships with possible drivers such as atmospheric circulations and SST changes are studied on local and global scales. The observed variations in cloud cover and the relationship between cloud cover and other variables are examined and compared with their variations simulated by the global climate models used in the IPCC AR4 in order to evaluate which of the model estimates of cloud feedback is the most reliable.

The characteristics of the climatological spatial distribution and temporal variation of cloud cover are examined using adjusted ISCCP data. Our results indicate that variations in low-level cloud cover are closely tied to variations in static stability, and indirectly related to variations in other parameters including divergence and the strength of the subtropical high. Based on our understanding of the environmental controls operating on cloud cover, we correlate cloud cover variations with variations in SST and other climatological variables including lower tropospheric stability (LTS), sea level pressure (SLP), and vertical velocity at 500hPa (W500). Each individual cloud type is differently correlated with SST. Low-level clouds are negatively correlated with SST over all oceans, while high-level clouds show positive correlation with SST, especially in the equatorial Pacific. The pattern of correlations shown for total cloud cover faithfully reflects the properties of both cloud types, i.e., negative correlation in the regions of persistent marine low-level cloud cover and positive correlation in the equatorial Pacific, where high-level clouds are dominant. Reductions in LTS

can be caused by increasing SST, which causes a decrease in cloud fraction by initiating a transition from low-level clouds to high-level clouds. High-level cloud cover shows significant opposite relationships with SST and LTS compared to low-level cloud cover. Therefore, the pattern of correlation for total cloud amount shows a positive correlation in regions of persistent marine low-level cloud cover and a negative correlation in the equatorial Pacific. In addition, low-level clouds are positively correlated with SLP over subtropical marine areas. This means that high pressure by subsidence is one of components related with the variations of low-level cloud cover. The correlations of the observed low-level cloud cover anomalies with a variety of variables suggest that low-level clouds in regions of persistent low-level clouds (tropical marine areas) are associated with a cool sea surface, stronger stability, higher sea level pressure, and subsidence. An increase in SST causes a reduction in lower tropospheric stability, which in turn allows for more vertical motion within and around the cloud deck that leads to increased dry air entrainment. This brings about a reduction in cloudiness and a transition from low-level cloud to high-level cloud types. Higher SLP can also produce more subsidence aloft and thereby increase LTS independent of SST.

To examine whether different GCMs can reliably replicate the observed variations in low-level cloud amount that are associated with certain meteorological variables, the pattern correlations of total cloud anomalies correlated with the local thermal structure (SST, LTS) and circulation (SLP, W500) are computed for each model. Most models poorly reproduce the general response of cloud cover to changes in meteorological variables. Only three models give pattern correlation coefficients over 0.4 for all variables, namely the CGCM3, GFDL_0, and HADCM3. CGCM3 well reproduces the observed spatial pattern of cloud response to the change in all variables, including the contrast response over the tropical Pacific and subtropical eastern oceans. The GFDL_0 and the HADCM3 show similar values for all variables, but they fail to capture the contrast structure over tropical ocean areas and the subtropical eastern oceans. Because evidence of low-level cloud cover in the cloud-meteorology correlation test occurs only in confined regions, the pattern correlation is not sufficient to determine whether the model shows the correct correlation relative to observations. The correlation between cloud cover and meteorological variables in the four cloud regions

are computed for each model and compared with observations to more closely examine the evidence for low-level cloud responses. The models are grouped according to whether they have the correct sign of correlation relative to observations. By successively eliminating models on this basis, we are left with only two models that simulate the correct sign of correlations for all variables, namely the CGCM3 and HADGEM1. These two models exhibit considerably good agreement with observations in terms of net cloud radiative forcing, including with the cooling and warming effects of shortwave and longwave radiation, respectively.

In this study, we give a concise answer to the question of whether low-level clouds act as a positive or negative feedback to climate change. The only two models in the CMIP3 archive that properly simulate clouds show a reduction in cloud cover throughout much of the Pacific in response to global warming by greenhouse gas forcing (i.e., a positive feedback). Evaluating cloud feedback with only two models is, however, far from ideal. This presents a clear challenge to develop a larger number of climate models that can pass these and other tests so that we may have greater confidence in the sign of the low-cloud feedback under future changes in greenhouse gas concentrations.

REFERENCES

Bony, S., et al., 2006: How well do we understand and evaluate climate change feedback processes? J. Climate, 19, 3445-3482.

Bony, S., and J.-L. Dufresne, 2005: Marine boundary-layer clouds at the heart of tropical cloud feedback uncertainties in climate models. Geophys. Res. Lett., 32(20), L20806, doi:10.1029/2005GL023851.

Campbell, G., 2004: View angle dependence of cloudiness and the trend in ISCCP cloudiness, paper presented at 13th Conference on Satellite Meteorology and Oceanography, Am. Meteorol. Soc., Norfolk, Va., 20-23 Sept.

Clement, A.C., R. Burgman, and J.R. Norris, 2009: Observational and model evidence for positive low-level cloud feedback. Science, 325, 460-464. Doi:10.1126/science.1171255.

Evan, A.T., A.K. Heidinger, D.J. Vimont, 2007: Arguments against a physical long-term trend in global ISCCP cloud amounts. Geophys. Res. Lett. 34, L04701, doi:10.1029/2006GL028083.

George, R. C. and R. Wood, 2010: Subseasonal variability of low cloud radiative properties over the southeast Pacific Ocean, Atmos, Chem. Phys., 10, 4047-4063, doi:10.5194/acp-10-4047-2010.

Jacobowitz, H., L.L.Stowe, G. Ohring, A.Heidinger, K. Knapp, and N.R.Nalli, 2003: The Advanced Very High Resolution Radiometer Pathfinder Atmosphere (PATMOS) climate dataset: a resource for climate research. Bull. Amer. Meteor. Soc., 84, 785-793.

Klein, S.A., and D. L. Hartmann, 1993: The seasonal cycle of low stratiform clouds. J. Climate, 6, 1587-1606.

Larson, K., D. L. Hartmann, and S. A. Klein, 1999: The role of clouds, water vapor, circulation, and boundary layer structure in the sensitivity of the tropical climate. J. Climate, 12, 2359–2374.

Meehl, G.A., C. Covey, T. Delworth, M. Latif, B. McAvyaney, J.F.B. Mitchell, R.J. Stouffer, K.E. Taylor, 2007: The WCRP CMIP3 multimodel dataset: a new era in climate change research. Bull. Amer. Met. Soc., 88, 1383-1394.

Norris, J.R., and C. B. Leovy, 1994: Interannual variability n stratiform cloudiness and sea surface temperature. J. Climate, 7, 1915-1925.

Norris, J.R., 2000: What can cloud observations tell us about climate variability? Space Sci. Rev. 94, 375-380.

Norris, J.R., 2005: Trends in upper-level cloud cover and surface divergence over the tropical Indo-Pacific Ocean between 1952-1997. J. Geophys. Res., 110, D21110, doi:10.1029/2005JD006183.

NRC (National Research Council), 2003: Understanding Climate Change Feedbacks. National Academies Press, Washington, DC, 152pp.

Ramaswamy, V. et al., 2001: Radiative Forcing of Climate Change, Chapter 6, pp.349-416.

Randall, D.A., et al., 2006: Cloud feddbacks. In: Frontiers in the Science of Climate Modeling [Kiehl, J.T., and V. Ramanathan (eds.)]. Proceedings of a symposium in honor of Professor Robert D. Cess.

Rossow, W.B., and R.A. Schiffer, 1999: Advances in understanding clouds from ISCCP. Bull. Am. Meteor. Soc., 80, 2261-2287.

Slingo, A. 1990: Sensitivity of the earth's radiation bedget to changes in low clouds. Nature, 343-49-51.

Soden, B. J., and I. M. Held, 2006; An assessment of climate feedbacks in coupled ocean-atmosphere models. J. Clim., 19, 3354-3360.

Stephens, G.L., 2005: Cloud feedbacks in the climate system: a critical review. J. Climate, 18, 237-273.

Stowasser, M., and K. Hamilton, 2006: Relationship between shorwave cloud radiative forcing and local meteorological variables compared in observations and several global climate models. J. Clim., 19, 4344-4359.

Webb, M.J., et al., 2006: On the contribution of local feedback mechanisms to the range of climate sensitivity in two GCM ensembles. Clim. Dyn., 27, 17-38.

Williams, K.D., M.A. Ringer, C.A. Senior. M.J. Webb, B.J. McAvaney, N. Andronova, S.Bony, J.-L. Dufresne, S. Emori, R. GuOhmura, T. Knutson, B. Li, K. Lo, I. Musat, J. Wegner, A. Slingo, and J.F.B. Mitchel, 2006: Evaluation of a component of the cloud response to climate change in an intercomparison of climate models. Clim. Dyn., 26, 145-165.

Wood, R., and D.L. Hartmann, 2006: Spatial variability of liquid water path in marine low clouds: The importance of mesoscale cellular convection. J. Climate, 19, 1748-1764.

Wyant, M.C., C.S. Bretherton, H. A. Rand, and D.E. Stevens, 1997: Numerical simulations and a conceptual model of the stratocumulus to trade cumulus transition. J. Atmos. Sci. 54, 169-192.

Wyant, M.C., C.S. Bretherton, J.T. Bacmeister, J.T. Kiehl, I.M. Held, M. Zhao, S.A. Klein, and B.J. Soden, 2006: A comparison of low-latitude cloud properties and their response to climate change in three US AGCMs sorted into regimes using mid-tropospheric vertical velocity. Clim. Dyn., 27, 261-279.

Wylie, D., D.L. Jackson, W. P. Mensel, and J.J. Bates, 2005: Trends in global cloud cover in two decades of HIRS ovservations. J. Climate. 18. 3021-3031.

Zhang, M., 2004: Cloud-climate feedback: how much do we know? In: Observation, Theory and Modeling of Atmospheric Variability, World Scientific Series on Meteorology of East Asia, Vol. 3 [Zhu et al. (eds)]. World Scientific Publishing Co., Singapore, 632pp.

APCC TECHNICAL REPORT 2011-03

- Model Evaluation for Low-Level Cloud Feedback
- Evaluation and Future Projection of Changes in Extreme Temperature and Precipitation Events
- Changes in East Asian Winter Monsoon

APEC Climate Center

12, Centum 7-ro, Haeundae-gu, Busan 612-020, Republic of Korea
Tel: +82-51-745-3900 Fax: +82-51-745-3949
www.apcc21.org

비매품
94500
9 788997 533159
ISBN 978-89-97333-18-9
ISBN 978-89-97333-15-8 (세트)